16th World Conference on Earthquake, 16WCEE 2017

Santiago Chile, January 9th to 13th 2017

Paper N° 4775

Registration Code: S-T1463209940

IN-PLANE SEISMIC FRAME ACTION EFFECTS ON BUCKLING-RESTRAINED BRACE WELDED END CONNECTION PERFORMANCE

J. Zhao[(1)], F. Lin[(2)], Z. Wang[(3)]

[(1)] *Associate Professor, State Key Laboratory of Subtropical Building Science, South China University of Technology, Guangzhou 510641, China, ctjxzhao@scut.edu.cn*

[(2)] *Xiamen BIAD Architecture Design Co., LTD, Xiamen 361009, China, linfuxiong2012@163.com*

[(3)] *Professor, State Key Laboratory of Subtropical Building Science, South China University of Technology, Guangzhou 510641, China, wangzhan@scut.edu.cn*

Abstract

In-plane buckling-restrained brace (BRB) end rotation induced by frame action is a commonly observed phenomenon in buckling-restrained braced frames (BRBFs). However, its effect on BRB end connection performance has not yet been clear. In this study, the frame action of non-moment-resisting braced frame was summarized based on previously observed BRBF responses. Four BRB end deformation modes for quick determination of BRB end rotational demand are proposed considering different BRB arrangements, the story where BRBs locate, and the boundary condition of corner gussets connected with column base. Key factors affecting BRB end rotation and BRB end moment are examined theoretically by parametric analysis. Subassemblage tests of four BRB specimens under horizontal cyclic loading were conducted by adopting two loading frames to impose the expected frame action effects. It shows that the BRB end rotation subjected the BRB ends to significant flexural moments, leading to premature yielding of the BRB ends or end zone buckling. The frame action effects and the flexural rigidity of BRB ends were found to have significant influence on BRB end connection performance. The triggering moment induced by the BRB end rotation was the main contributor to BRB end moment. However, the moment amplification effect induced by the flexure of BRB end zones became prominent especially for small flexural rigidity of BRB ends.

Keywords: buckling-restrained brace; frame action; connection; rotation; end moment

1. Introduction

Buckling-restrained braces (BRBs), viewed as high performance metallic yielding dampers [1-5], have been widely implemented into engineering structures to mitigate structural damage. Generally, axial yielding of a BRB (Fig.1 (a)) is only allowed within the plastic zone, while the end zones projected from the casing are required to remain elastic to ensure stability of the connections. In actual applications, BRB-to-gusset connection by full penetration groove weld (Fig.1(a)) is quite popular, with the advantage of higher strength and easier construction than bolted and pinned end connections. Another type of welded end-slot connection for BRBs was also proposed recently [6] and has gained wide acceptance in Taiwan. With such a welded (bolted) BRB end, rigid-body rotation (θ_t and θ_b in Fig.1 (b)) between the end zone and the plastic zone would be inevitable under the in-plane frame action effects (H and R in Fig.1 (b)). Previous subassemblage [7-9] and frame tests [10] showed that such BRB end rotational demands could be comparable to the inter-story drift angle, making the BRBs and their connections more susceptible to unexpected failure than pure axial loading condition.

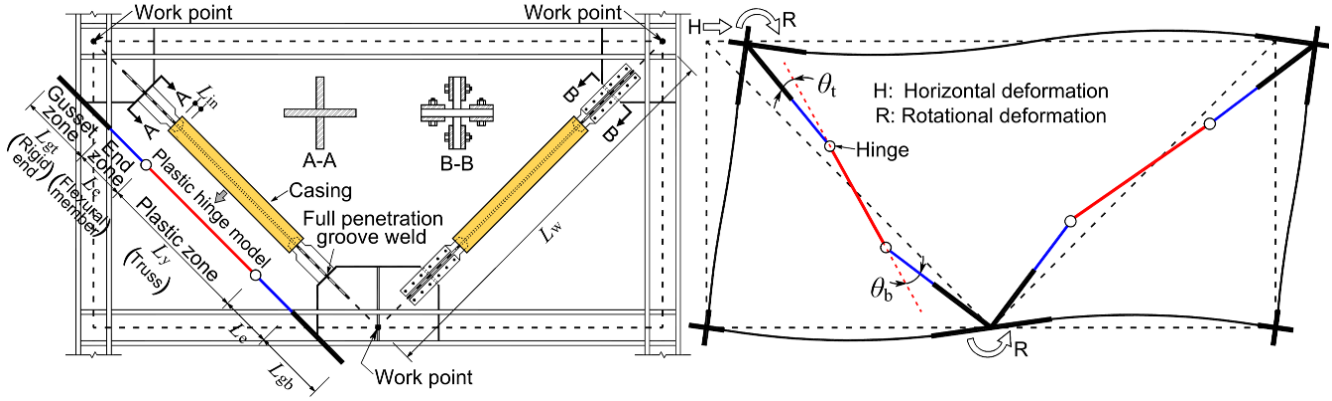

Fig. 1 –BRB end rotation induced by one typical in-plane frame action

Saeki et al. [11] conducted component tests of practical-scale BRBs with cruciform bolted end connections. The BRB was assumed as a continuous elastic flexural member to estimate the in-plane frame-induced secondary moments on BRB ends. The BRB specimens were placed vertically with fixed bottom end, while an equivalent eccentricity of 20 to 80 mm was applied, respectively, onto the top end of the specimens to simulate the secondary moments. Test results showed that plastic hinge formed at the neck of the projected end zone shortly after compressive yielding of the core members. This behavior led to premature buckling of the entire BRB end connections that failed to develop full hysteresis of BRBs. Uemura et al. [12] conducted subassemblage tests to simulate more realistic frame action effects on the BRBs with cruciform welded end connections. The bottom gusset plate of the specimens was fixed onto the strong floor while both horizontal and rotational deformations were imposed onto the top gussets through a pin-ended rocking column. Test results showed that plastic hinge formed at the BRB-to-gusset section that caused in-plane buckling of the entire connection prior to 2% drift. However, the connections all satisfied the required axial strength capacity considering the maximum BRB compressive force. The two studies [11,12] highlighted the negative effect of frame-induced secondary moments on the in-plane BRB end connection performance. On the other hand, many frame tests [13-18] also demonstrated the negative frame action effect on BRB corner gusset connections. It was found that the beam and column seismic shear forces would cause the beam-column-gusset joint opening or closing under repeated loading. Such behavior would introduce diagonal strut force on the gusset-to-beam and gusset-to-column interfaces, making the corner gusset more susceptible to fracture at the gusset tip, or out-of-plane buckling when BRBs were still in tension.

Based on the above summary, it is clear that the interaction between braced frame deformation and BRB end connection behavior has been one of the most concerned issues. Although the flexural moment induced by end rotation was found to be responsible for buckling failure of BRB end zone [12], several issues still remain unclear and need to be addressed to gain further insights: 1) key factors affecting the relationship between braced

frame deformations and BRB end rotation, 2) key factors affecting BRB end rotational and flexural behavior, and theoretical predictions for their peak demands, and 3) effective ways to minimize the negative effect of braced frame deformations on the BRB end zone behavior. Note that moment or non-moment frame can be used in buckling-restrained braced frame (BRBF). It is also known that flexible beam-to-column connections would be a better alternative to improve the seismic performance of BRBF. Hence, the frame action of non-moment-resisting braced frame is only discussed in this study. In the following sections, four BRB end deformation modes are summarized from previously tested BRBF responses. Theoretical predictions of BRB end rotation and flexural moments for different deformation modes are proposed. Parametric analysis is performed to examine the key factors affecting the rotational and flexural demands. Subassemblage tests were then conducted on four BRB specimens with welded end connections to verify the theoretical predictions. Implications for considering and minimizing the negative effect of braced frame deformations in BRB end connection design are summarized finally.

2. Theoretical study on frame-induced BRB end moments

2.1 Frame action effects on BRB ends

The three-story three-bay CFT/BRB frame test by Tsai et al. [10] is first reviewed to examine the characteristics of braced frame deformations. As shown in Fig.2, flexible beam-column connections were adopted in the middle bay. It was found that the rotational responses of the central gussets were rather minor by the release of beam end moments. For the corner gussets connected with the 2nd and 3rd floors, their responses were comparable with the inter-story drift angle. It is because the corner gussets were flexurally isolated from beam ends and welded to the interior columns only. On the other hand, the corner gussets on the ground floor were welded to the column base which was completely embedded into the foundation to represent fix-ended condition. It was observed that their rotational responses were reduced to be about 1/3 of the inter-story drift angle.

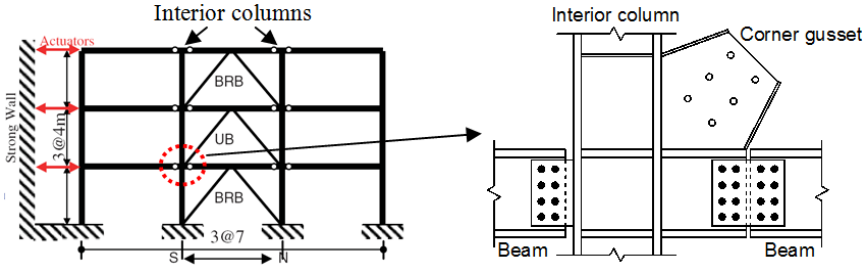

Fig. 2 –Details of non-moment-resisting braced frame by Tsai et al. [10]

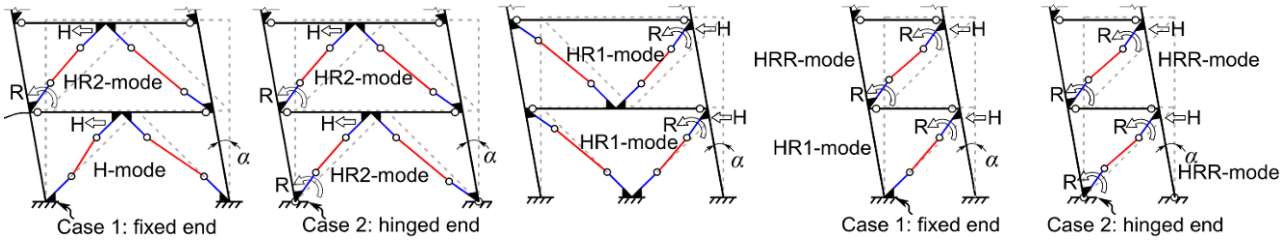

(a) Chevron (b) V-type (c) Single-diagonal

Fig. 3 –Rigid-body configuration of BRBs induced by non-moment frame action

Based on these previously observed responses, Fig.3 summarizes the expected rigid-body deformations of BRBs with varous arrangements in non-moment-resisting braced frame. For the first story BRBs with chevron and single-diagonal arrangements, two extreme cases, i.e. hinge- and fix-ended boundary conditions, are considered for the gusset-and-column assemblies. Therefore, four typical frame action effects on BRB ends can be concluded, i.e. H-mode (without any rotation on both ends), HR1-mode (with rotation on the top end only), HR2-mode (with rotation on the bottom end only), and HRR-mode (with rotation on both ends). Note that the

HR1-and HR2-modes are actually the same for the case of symmetric gusset zone. From these configurations, it is clear that the BRB end connections would be subjected to additional end moments which relates to specific BRB end rotational demands. Therefore, correlation among braced frame deformation, BRB end rotation and BRB end moments needs to be discussed.

2.2 Theoretical BRB end moments

As shown in Fig.4, γ_t and γ_b are the rotation of gusset zone induced by frame action; φ_t and φ_b are the initial rotation of gusset zone due to geometric imperfections; α is the inter-story drift angle. Counterclockwise rotation of these parameters is defined as negative. Rigid ends are assumed within the gusset zones while two rotational springs with a rotational rigidity K_R are provided at the BRB-to-gusset sections to represent the semi-rigid behavior. The end zone and plastic zone are simplified as a flexural and an axial compression member, respectively, with a hinge connection in between. This model was found appropriate when the insert length of end zone L_{in} (see Fig.1 (a)) is smaller than the core plate width [19], commonly found in actual applications.

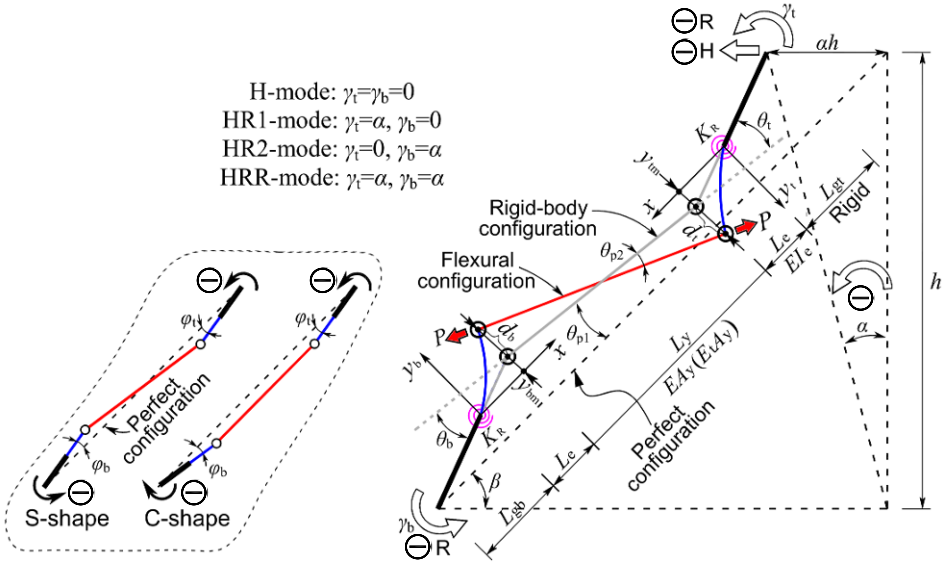

(a) Initial geometric imperfections (b) Analytical model

Fig. 4 –Analytical model of BRB end connections

Based on rigid-body motion analysis, the rigid-body end rotation, θ_t and θ_b, and the relative plastic zone rotation between the rigid-body and the geometrically perfect configurations, θ_{p1}, can be given by

$$\theta_t = (\gamma_t + \varphi_t)(1 + a_{ey} + a_{gty}) + (\gamma_b + \varphi_b)(a_{ey} + a_{gby}) - \alpha(\sin^2\beta)/a_{yw} \quad (1)$$

$$\theta_b = (\gamma_t + \varphi_t)(a_{ey} + a_{gty}) + (\gamma_b + \varphi_b)(1 + a_{ey} + a_{gby}) - \alpha(\sin^2\beta)/a_{yw} \quad (2)$$

where β=inclined angle of BRB, $L_w=L_y+2L_e+L_{gt}+L_{gb}$=total length between work points, $a_{ey}=L_e/L_y$, $a_{yw}=L_y/L_w$, $a_{gty}=L_{gt}/L_y$, $a_{gby}=L_{gb}/L_y$. Particularly, $a_{gty}=a_{gby}=(1/a_{yw}-1)/2-a_{ey}$ can be obtained for symmetric gusset zone ($L_{gt}=L_{gb}$). The values of γ_t and γ_b are summarized in Fig.4 based on the frame action in Fig.3. The initial rotation of $|\varphi_t|=|\varphi_b|=1\%$, superposed on the same rotational direction of the corresponding BRB end, is recommended to be considered. By taking moment equilibrium at the BRB-to-gusset section, the total end moments can be given by

$$M_t = P\theta_t L_e + P[(1 + a_{ey})d_t + a_{ey}d_b] = M_{tr,t} + M_{a,t} \quad (3)$$

$$M_b = P\theta_b L_e + P[a_{ey}d_t + (1 + a_{ey})d_b] = M_{tr,b} + M_{a,b} \quad (4)$$

where $M_{tr,t}$ and $M_{tr,b}$ are the triggering moments of the top and the bottom ends, respectively, induced by rigid-body rotation only. $M_{a,t}$ and $M_{a,b}$ are the amplified moment caused by bending of the entire connection.

From Eqs. (3) and (4), it is seen that the total end moment is the combination of the triggering moment and the amplified moment. The triggering moment can be obtained from Eqs. (1) and (2) once the frame action effects and BRB geometry have been determined. Note that d_t and d_b relate to both the bending stiffness of BRB end zone and the rotational rigidity at the BRB-to-gusset section. Such a rotational rigidity is governed by specific BRB-to-connection details and difficult to be predicted theoretically. Therefore, the contributions of the amplified moment is evaluated in this paper by substituting the experimental d_t and d_b responses into $M_{a,t}$ and $M_{a,b}$.

2.3 Parametric analysis on BRB end rotation and triggering moment

The theoretical relationship between BRB end rotation and inter-story drift angle, governed by Eqs. (1) and (2), is presented in Fig.5. The solid and dashed lines mean the top and bottom end responses, respectively. Also presented are the rigid-body configurations of BRBs at -3% drift. The frame action effects (Fig.3) governed by the HRR- and the HR1-modes are to be discussed herein.

It shows that the responses grow significantly with the increase of α and the decrease of a_{yw}, indicating that the increase of connection zone length would be unfavorable. For the HRR-mode, the two BRB ends rotate in a counterclockwise S-shape configuration and their peak responses grow significantly with the decrease of BRB inclined angle β. For the HR1-mode with β=45°, the BRB ends always rotate in a symmetric C-shape configuration with a fixed response of 0.5α. For the HR1-mode with β=30° and 60°, the two ends deformed from C-shape into S-shape with the decrease of a_{yw}, and their peak responses ranges from 0.9 to 1.3α. Apparently, these two cases are more unfavorable than β=45°. Compared with the HR1-mode, the peak responses of the HRR-modes are more unfavorable for $\beta \leq 45°$. The above analysis confirmed that the BRB end rotation and triggering moment are governed by frame action effects and BRB geometry, which should be properly considered in design. These responses are expected to grow if the initial imperfections corresponding to the rotational configurations of BRBs (C- or S-shape) are incorporated.

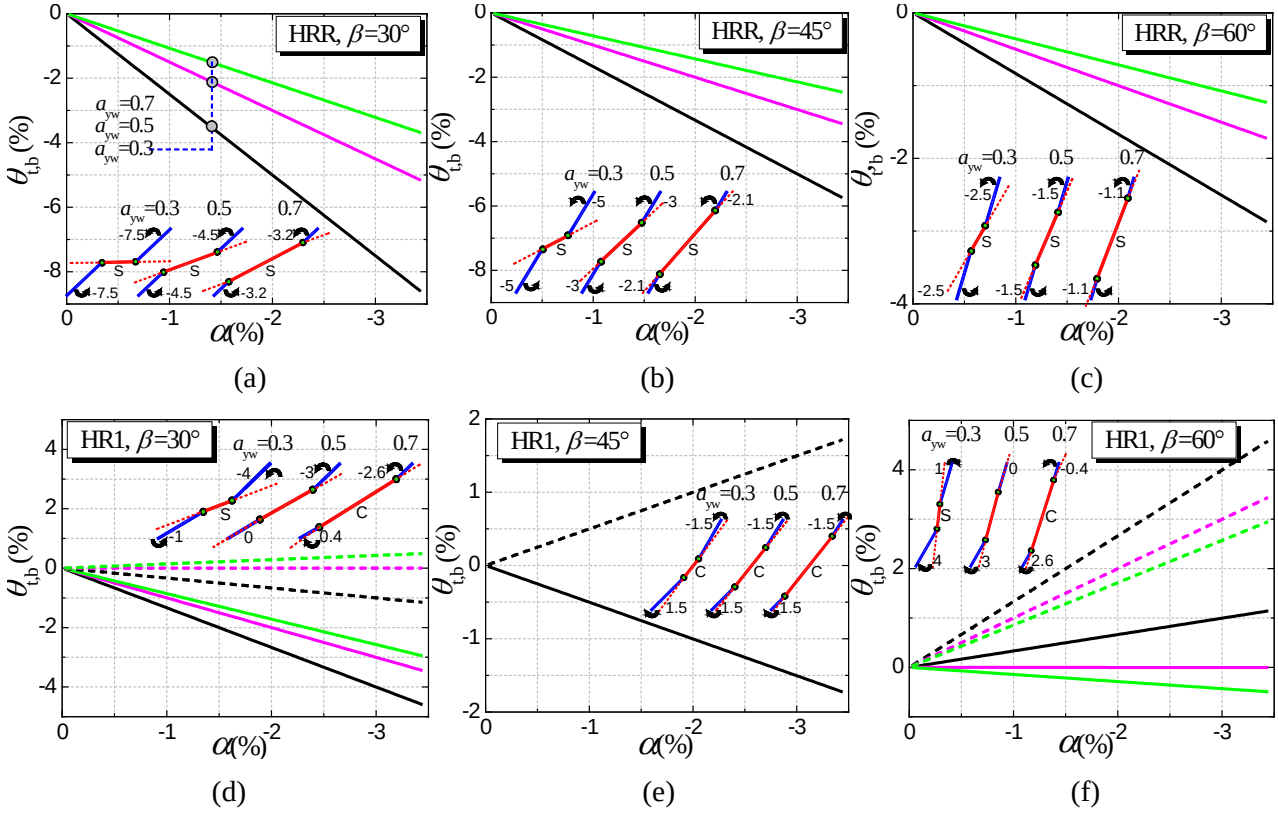

Fig. 5 –Effect of frame action and BRB geometry on BRB end rotation

3. Subassemblage test program

3.1 Specimens

Subassemblage tests to similuate different frame action effects on BRB end connection were conducted in order to verify the above analytical conclusions and gain more insights into the in-plane BRB end connection performance. Four BRB specimens with welded end connections were designed. Configurations and material properties of the specimens are illustrated in Fig.6 and Table 1, respectively.

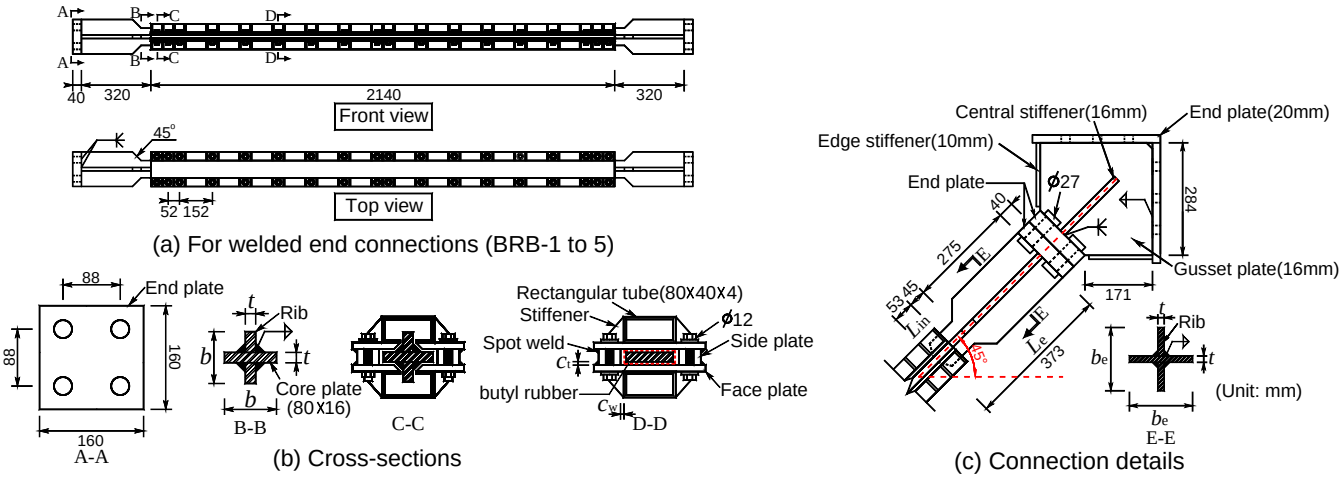

Fig. 6 –Configuration of BRB specimens and connection

Table 1– Material properties of specimens

Category	Material grade	Yield strength f_y (MPa)	Tensile strength f_u (MPa)	Elastic modulus E (MPa)	Elongation (%)
Steel core and gusset plate	Q235-B	256	426	2.0×105	36

Table 2– Actual geometric dimensions and parameters of the specimens

Specimen No.	b_e (mm)	Frame action	P_y (kN)	a_{yw}	β	Connection type	A_e/A_y	P_{ej}/P_y
BRB-1	99.2	HR1	318	0.5	45°	Weld	2.3	15
BRB-2	119.5	HR1	324	0.5	45°	Weld	2.8	25
BRB-3	99.6	HRR	324	0.5	45°	Weld	2.3	15
BRB-4	119.5	HRR	322	0.5	45°	Weld	2.8	25

The sandwiched all-steel BRB configuration was adopted to simplify BRB fabrication. The steel core consisted of a 80×16mm core plate as the plastic zone with the designed length of 2034 mm. A 0.5 mm-thick layer of butyl rubber was attached onto the plastic zone to minimize the friction induced by high-mode buckling of the core plate. The steel core was sandwiched by two welded steel components and two side plates using high-strength bolts. The nominal gap, c_t=1mm and c_w=1.5mm, was provided to accommodate the expansion of plastic zone due to the Poisson's effect. To ensure stable hysteretic behavior, the buckling amplitude of core plate, governed by c_t and c_w also, was well controlled to be smaller than 4% of the buckling half-wave length of the core plate by assuming its tangent modulus E_t=1%E [20]. Cruciform gusset plate with edge stiffeners was designed. To facilitate replacement of the specimens from the gusset connection, two 40 mm-thick end plates

were welded to the end of BRB and gusset plate, respectively, so that they could be connected by four high-strength bolts. The gusset plate was also welded to two 20 mm-thick end plate for bolted connection to the loading frame. The key parameters of the specimens include the width b_e of the BRB end zone and the frame action effects on BRB ends, while the axial yield force and overall BRB geometry were fixed. The change of b_e also leads to a variation of the cross-sectional area and bending stiffness of the end zone, represented by A_e/A_y and P_{ej}/P_y, respectively. A_y and A_e are the cross-sectional areas of the plastic zone and end zone, respectively. $P_{ej}=\pi^2 EI_e/(2L_e)^2$ is the Euler buckling strength of the end zone assuming one end fixed and the other one free. P_y is the yield force of BRB.

3.2 Test setup

To examine the effect of BRB end deformation modes, two loading frames were designed based on the parameters of the specimens (Table 3). For the HR1-mode (Fig.9 (a)), the bottom ends of the two columns were pin-connected with the bottom beam. The bottom end of the left column was also fixed with a rotation-locking support by high-strength bolts so that a fix-ended condition could be achieved. The top end of the right column was welded to a loading beam, which was horizontally connected to the reaction wall by two MTS actuators. With this configuration, both horizontal and rotational deformations could be imposed on the top gusset only, corresponding with the HR1-mode. For the HRR-mode (Fig.9 (b)), the rotation-locking support was detached from the above loading frame while an additional top beam was connected to the top ends of the two columns by pins. This new configuration could impose the same rotational deformation on the top and bottom gussets, corresponding with the HRR-mode. Four lateral cables were mounted onto the two columns to ensure out-of-plane stability.

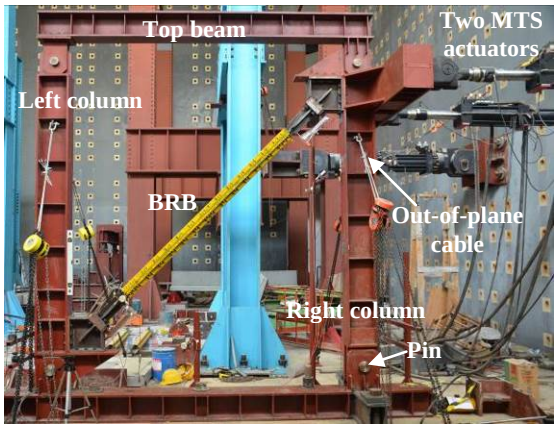

(a) Loading frame for HRR-mode

(b) Loading frame for HR1-mode

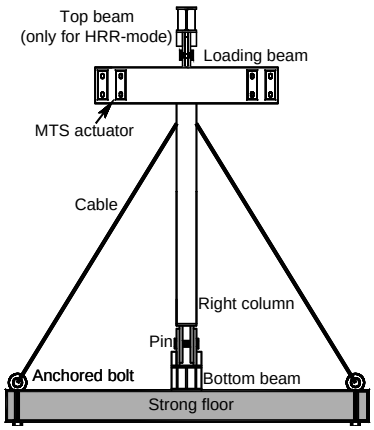

(c) Cables to ensure Out-of-plane stability

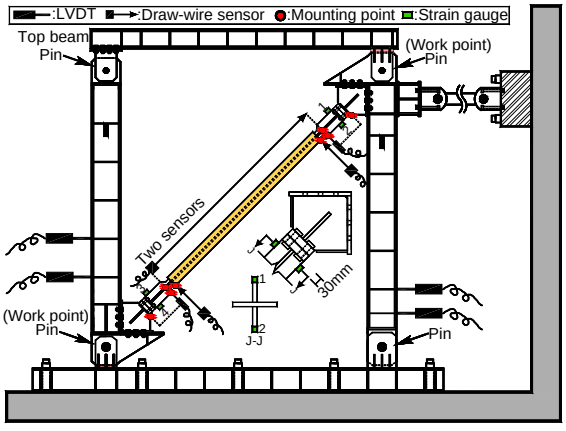

(d) Instrumentation

Fig. 7 –Test setup and instrumentation

Two displacement transducers (LVDT) were placed perpendicularly to the two columns to measure the inter-story drift angle α. Two draw-wire sensors were placed perpendicularly to the casing and mounted on its two ends to measure the in-plane rotational behavior of plastic zone. Obviously, the rotational behavior of the two gussets should be identical with their adjacent columns. Therefore, BRB end rotation θ_t and θ_b, induced from the loading frame deformations, could be obtained by subtracting the measured rotation of the column and the plastic zone. Strain gauges, labeled No.1 to No.4, were attached closely to the welded section of BRB end (30mm away to avoid strain concentration) or on the splice plate section to examine the flexural moments. Two LVDTs were mounted between the edge stiffeners of gussets and the ends of core transition zone to measure the flexural deformations of the end zones projected outside the casing. Two draw-wire sensors were mounted between the two ends of core transition zone to measure the BRB axial deformation δ.

Incremental cyclic tests were conducted at the Structural Engineering Laboratory of Guangdong University of Technology. Loading at $0.5P_y$ with 2 cycles (Step 1) was first applied to examine the initial geometric imperfections. For elasto-plastic range, the axial deformation δ was taken as the controlled displacement, which could be approximated by:

$$\delta = \alpha \frac{L_w}{2} \sin(2\beta) \tag{5}$$

Assuming α=0.5% (Step 2), 1% (Step 3), 1.5% (Step 4), 2% (Step 5), 2.5% (Step 6) and 3% (Step 7), the imposed axial deformations would be 10.2mm (2 cycles), 20.3mm (2 cycles), 30.5mm (2 cycles), 40.7mm (5 cycles), 50.8mm (2 cycles) and 61mm (≥1 cycle), respectively. Owing to the elastic axial deformation of BRB end and gusset plate, the measured inter-story drift angle of the loading frame would be slightly larger than the expected drift responses.

4. Test results and analysis

4.1 Cyclic behavior of BRB

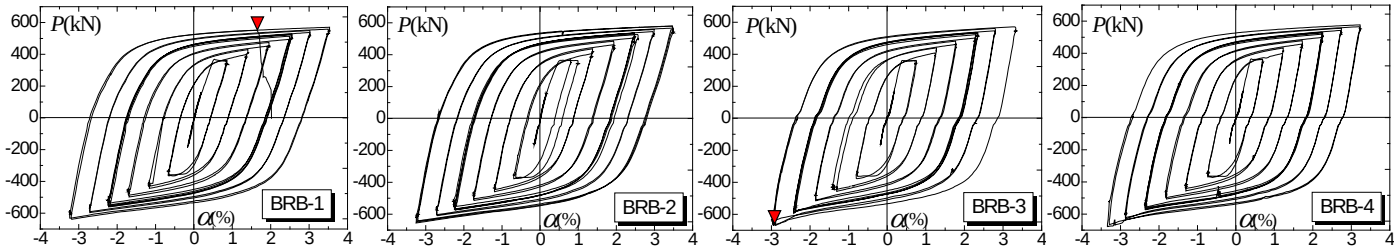

Fig. 8 –Axial force of BRB vs. inter-story drift response

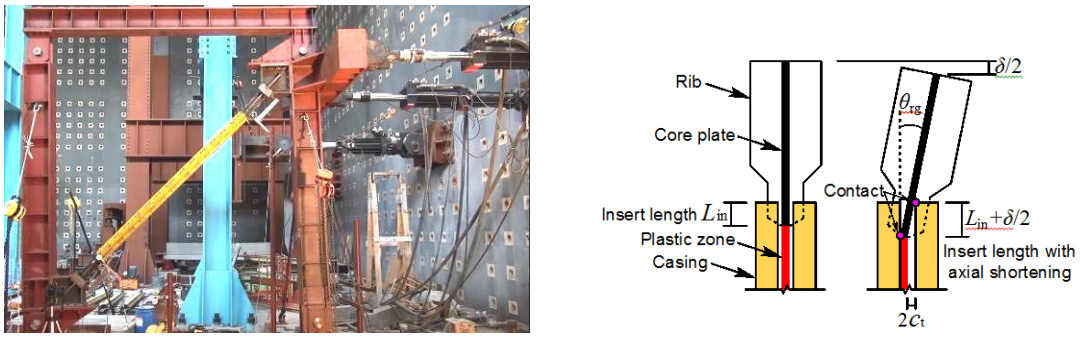

(a) Global failure (b) Local interaction between casing and BRB end

Fig. 9 –Failure mode of BRB-3 due to BRB end buckling

Fig.8 shows the cyclic behavior of BRB using the axial force vs. the inter-story drift responses. Failure of the specimens is indicated with shaded triangle. BRB-1 and 3 exhibited tensile rupture and compressive buckling (Fig.9) during the excursion of 3% loading, while BRB-2 and 4 remained stable at all loading cycles. In general,

specimens all exhibited full and stable cyclic performance, indicating that braced frame deformations did not seem to have significant effects on the BRB hysteretic behavior. However, compared with BRB-1 and 2, the compression strength hardening effect was observed for BRB-3 when the imposed drifts reached between 2% and 3%. This should be due to the additional friction between the inserted end zone and the casing end when buckling of the BRB end tended to occur to cause two-point contact (Fig.9).

4.2 Flexural behavior of BRB end connections

Fig.10 shows the experimental and theoretical BRB end rotational responses (Only the larger end responses are presented). The initial rotation induced by initial geometric imperfections is also included into the theoretical and measured responses. Also presented are the deformed rotational configurations at -3% drift. The negative sign means counterclockwise rotation. The peak responses of BRB-3 and 4 were more than twice of BRB-1 and 2, indicating that the HRR-mode imposed on BRB-3 and 4 would be more unfavorable. Also, the BRB end rotation almost showed linear relationship with the inter-story drift. The experimental responses could be well captured by the proposed predictions for the HRR-mode. Although some differences could be observed between the theory and the experiment for the HR1-mode, their developing trends were similar. Generally, the proposed predictions for BRB end rotation (Eqs. (1) and (2)) can be confirmed.

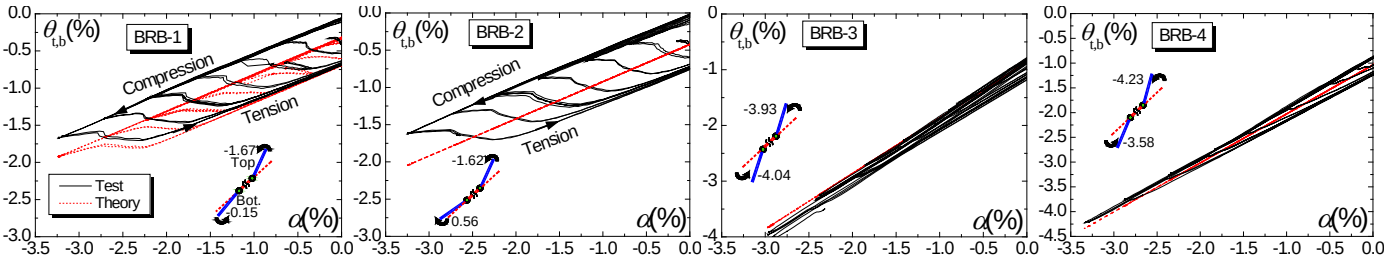

(a) BRB-1 top (b) BRB-2 top (c) BRB-3 bottom (d) BRB-4 top

Fig. 10 –BRB end rotation vs. inter-story drift response

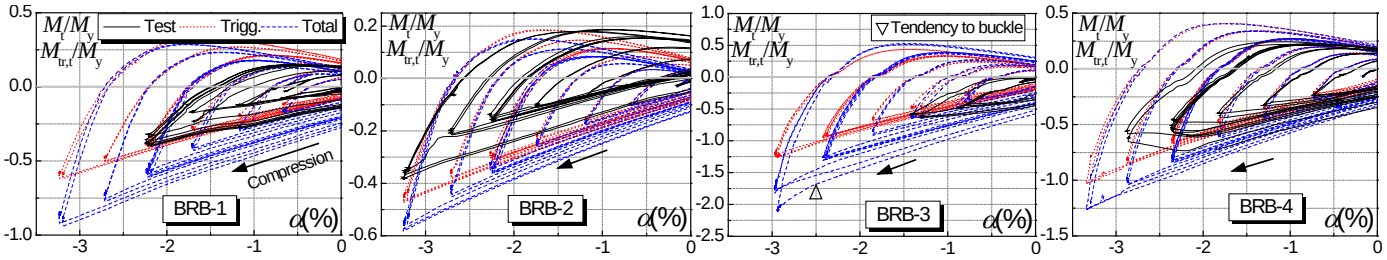

(a) BRB-1 top (b) BRB-2 top (c) BRB-3 top (d) BRB-4 top

Fig. 11 –Comparison between experimental and theoretical BRB end moments

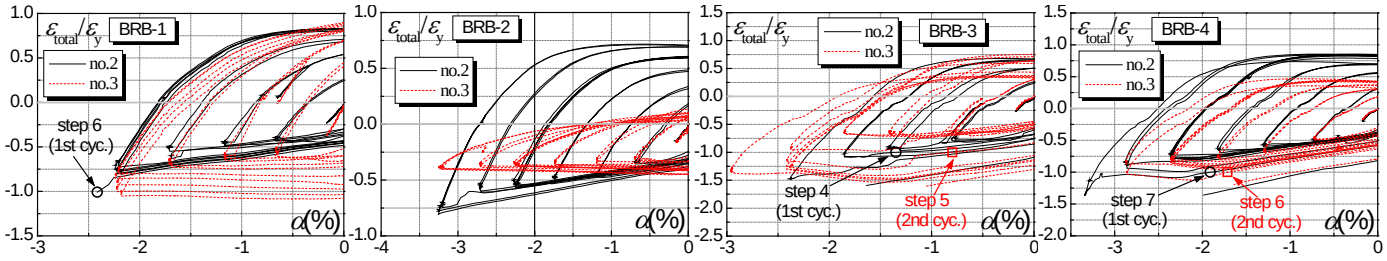

(a) BRB-1 (b) BRB-2 (c) BRB-3 (d) BRB-4

Fig. 12 –Experimental strain responses

Based on the above responses, the theoretical BRB end moments can be determined from Eqs. (3) and (4) and presented in Fig.11 (Only the larger responses of the two ends are presented). The measured flexural deformations d_t and d_b in the tests are incorporated into the two equations to obtain the total end moments. Counterclockwise moment is defined as negative. Also presented in Fig.11 is the experimental response calculated by strain gauge values within elastic stage. In general, the trends and amplitudes of the experimental

responses could be roughly estimated by the theoretical ones. The triggering moment was always the main contributor to the total end moments. Particularly for BRB-3, the developing trend of its top end responses significantly rose when α approached -2.5%, characteristic of end zone buckling. This indicates a remarkably negative effect of braced frame deformations on BRB end zone. Comparing BRB-1 and 3 and BRB-2 and 4, the negative effect of HRR-mode was also evident, verifying the predictions in Fig.5 (b) and (e). For BRB- 4, the measured responses started to fall when α exceeded 2%. This could be explained by the two point contact behavior near casing end which introduced opposite moments to those induced by BRB end rotation.

Fig.12 shows the total strain responses ε_{total} normalized with the yield strain ε_y to identify the occurrence of yielding and evaluate different plastic deformation demands among specimens. Only the strain responses within normal-functioning range are presented and the negative sign denotes compression. The strain responses at the most unfavorable strain gauge location (i.e. the flexural and axial strains were both negative under BRB compression) are only plotted. Initial yielding of the specimens are also marked by circle and square for the top and bottom ends, respectively. It is seen that plastic responses were observed for BRB-1, 3 and 4 with the maximum $\varepsilon_{total}/\varepsilon_y$ value of -1.61 (BRB-3). For BRB-3 and 4, premature yielding was observed during the 1.5% and 2.5% loading step, respectively. This indicates that braced frame deformations would subject BRB ends to premature yielding under the combined effect of axial compression and flexure. Similarly, the negative effect of HRR-mode and potential beneficial effect of two-point contact behavior were also evident.

5. Conclusions

The effect of non-moment-resisting braced frame seismic deformations on the in-plane BRB end connection performance was investigated theoretically and experimentally in this paper. Main conclusions can be drawn as follows:

1) Four BRB end deformation modes, H, HR1, HR2 and HRR, are proposed conceptually to enable quick determination of BRB end rotational demand and triggering moment.

2) BRB end rotation, induced by braced frame deformations, would subject BRB end zone to in-plane flexural moment, leading to premature yielding of BRB ends and tendency of end zone buckling. This kind of bending effect should be carefully considered in design.

3) The frame action effects and flexural rigidity of BRB end zone have significant effects on BRB end structural behavior. Test confirmed that the BRB ends with small flexural rigidity were prone to experience premature yielding. For the BRB with an inclination of 45° with a plastic zone length ratio of 0.5, HRR-mode were more unfavorable than HR1-mode.

4) Triggering moment was found to be the main contributor to BRB end moment. Parametric analysis shows that reducing the length of connection zone is always effective to minimize BRB end moments.

5) Test results showed that the amplified moment may have significant effect on BRB end moment especially for the BRB end having small flexural rigidity. Analytical prediction of the moment amplification factor considering the combined effect of frame action and flexural rigidity of BRB end is indispensable for design.

6) The initial geometric imperfection was found to have significant effects on BRB end flexural behavior. The imperfection shape matching the expected BRB end rotation mode is recommended to be considered.

6. Acknowledgments

This research is funded by the National Natural Science Foundation of China (Grant No. 51408226), the Guangdong Young Talent Project of Science and Technology Innovation (Grant No. 2014TQ01Z429), the Pearl River S&T Nova Program of Guangzhou (Grant No. 201610010075), and the Specialized Research Fund for the Doctoral Program of Higher Education (Grant No. 20130172120012).

7. References

[1] Black CJ, Makris N, Aiken ID (2004): Component testing, seismic evaluation and characterization of buckling-restrained braces. *Journal of Structural Engineering, ASCE*, 130(6): 880-894.

[2] Iwata M, Murai M (2006): Buckling-restrained brace using steel mortar planks: performance evaluation as a hysteretic damper. *Earthquake Engineering and Structural Dynamics*, 35: 1807-1826.

[3] Tremblay R, Bolduc P, Neville R, DeVall R (2006): Seismic testing and performance of buckling-restrained bracing systems. *Canadian Journal of Civil Engineering*, 33: 183-198.

[4] Ding YK, Zhang YC, Zhao JX (2009): Tests of hysteretic behavior for unbonded steel plate brace encased in reinforced concrete panel. *Journal of Constructional Steel Research*, 65: 1160-1170.

[5] Palazzo G, López-Almansa F, Cahís X, Crisafulli F (2009): A low-tech dissipative buckling restrained brace. Design, analysis, production and testing. *Engineering Structures*, 31: 2152-2161.

[6] Tsai KC, Wu AC, Wei CY, Lin PC, Chuang MC, Yu YJ (2014): Welded end-slot connection and debonding layers for buckling-restrained braces. *Earthquake Engineering and Structural Dynamics*, 43(12): 1785-1807.

[7] Zhao JX, Lin FX, Wang Z (2016): Effect of non-moment braced frame seismic deformations on buckling-restrained brace end connection behavior: Theoretical analysis and subassemblage tests. *Earthquake Engineering and Structural Dynamics*, 45(3): 359-381.

[8] Nishimoto K, Nakata Y, Kimura I, Aiken I, Yamada S, Wada A (2004): Sub-assembly testing of large buckling-restrained unbonded braces. *13th world conference on Earthquake Engineering*, Vancouver, Canada.

[9] Qu Z, Kishiki S, Sakata H, Wada A and Maida Y (2013): Subassemblage cyclic loading test of RC frame with buckling restrained braces in zigzag configuration. *Earthquake Engineering and Structural Dynamics*,42: 1087-1102.

[10] Tsai KC, Hsiao PC (2008): Pseudo-dynamic test of a full-scale CFT/BRB frame—Part II: Seismic performance of buckling-restrained braces and connections. *Earthquake Engineering and Structural Dynamics*, 37: 1099-1115.

[11] Saeki E, Maeda Y, Iwamatsu K, Wada A (1996): Analytical study on unbounded braces fixed in a frame. *Journal of Structural and Construction Engineering, Architectural Institute of Japan*, 489: 95-104 [in Japanese].

[12] Uemura K, Fujisawa K, Shimizu T, Inoue K (1997): Design method to prevent buckling of low yield strength steel tube brace and fracturing of joints (Part 2: Test results of braced braces). *Summaries of Technical Papers of Annual Meeting, Architectural Institute of Japan*, 9: 783-784 [in Japanese].

[13] Aiken ID, Mahin SA, Uriz P (2002): Large-scale testing of buckling-restrained braced frames. *Proceeding of Japan Passive Control Symposium*, Tokyo, Japan.

[14] Kaneko K, Kasai K, Motoyui S, Sueoka T, Azuma Y, and Ooki Y (2008): Analysis of beam-column-gusset components in 5-story value-added frame. *Proceeding of the 14th World Conference on Earthquake Engineering*, Beijing, China.

[15] Kishiki S, Uekusa M, Wada A (2008): Experimental evaluation of structural behavior of steel member affected by the presence of gusset plate (Part 2: Global enhancement of seismic performance of passive-controlled structures). *Journal of Structural and Construction Engineering, Architectural Institute of Japan*, 73: 2027-2036 [in Japanese].

[16] Chou CC, Liu JH, Pham DH (2012): Steel buckling-restrained braced frames with single and dual corner gusset connections: seismic tests and analyses. *Earthquake Engineering and Structural Dynamics*, 41: 1137-1156.

[17] Lin PC, Tsai KC, Wu AC, Chuang MC (2014): Seismic design and test of gusset connections for buckling-restrained braced frames. *Earthquake Engineering and Structural Dynamics*, 43: 565-587.

[18] Lin PC, Tsai KC, Wu AC, Chuang MC, Li CH, and Wang KJ: Seismic design and experiment of single and coupled corner gusset connections in a full-scale two-story buckling-restrained braced frame. *Earthquake Engineering and Structural Dynamics*, DOI: 10.1002/eqe.2577

[19] Takeuchi T, Ozaki H, Matsui R, Sutcu F (2014): Out-of-plane stability of buckling-restrained braces including moment transfer capacity. *Earthquake Engineering and Structural Dynamics*, 43: 851-869.

[20] Zhao JX, Wu B, Li W, Ou JP (2014): Local buckling behavior of steel angle core members in buckling-restrained braces: Cyclic tests, theoretical analysis, and design recommendations. *Engineering Structures*, 66: 129-145.